J Inno Sci Eng, 2022, 6(2):279-296
http://www.doi.org/10.38088/jise.1078914

Research Article

Influence of Bridge Piers on Velocity under Unsteady Flows

Gokcen Bombar

İzmir Katip Çelebi University, Department of Civil Engineering, Çiğli, İzmir, Turkey.

Cite this paper as:
Bombar, G. (2022). *Influence of Bridge Piers on Velocity under Unsteady Flows.* Journal of Innovative Science and Engineering. 6(2): 279-296

*Corresponding author: Gokcen Bombar
E-mail: gokcen.bombar@ikcu.edu.tr

Received Date: 25/02/2022
Accepted Date: 24/08/2022

Abstract

It is reported that every year hundreds of bridges collapse due to the dynamic forces acting on the piers, particularly during floods and the scour around the foundations. Since the determination of the velocity distribution upstream of the pier is directly related to this force, it is important to predict the effect of a presence and diameter of a bridge pier on velocity and turbulence parameters. In this study, the time variation of point velocities in the stream-wise and vertical direction at a point upstream of a bridge pier was obtained under clear-water and unsteady flow conditions. The presence of the bridge pier causes the velocity profile to be steeper. The increase in pier diameter decreased the maximum stream-wise velocity whereas it increased the vertical velocity in the down flow direction particularly near the bed. The turbulence intensity in stream-wise direction increases in the rising limb and decreases in the falling limb, more prominently near the bottom. The maximum percent reductions in the stream-wise velocities at peak flow were calculated as 6% and 11% for the small and big piers, respectively. The reduction in stream-wise velocity at peak flow increases with depth especially for the pier with greater diameter.

Keywords: Flood flow, Bridge pier, Velocity time series, Velocity profile.

1. Introduction

The collapse of a bridge usually results in a loss of life and property where almost 60% of these failures result from scour and other hydraulic-related causes [1]. Especially, after a heavy rainfall inducing a flood flow, the dynamic forces acting on the piers increase rapidly which are directly related to the velocity and its vertical distribution [2]. Therefore, the stability and structural design of bridges must be obtained from the velocity distribution at the upstream of the pier, to predict the drag forces correctly, principally when the velocity is not constant but a function of time.

Since the bridge pier in the flow acts as an obstacle, the flow decelerates as it approaches the pier and it is reduced to zero on the upstream side of the pier [3, 4]. The velocity flow field and turbulence parameters in steady flows around bridge piers have been investigated by many researchers both experimentally [5, 6] and numerically [7, 8]. Baker[9, 10, 11] and Yulistiyanto [12] obtained the stream-wise and vertical velocity components, turbulence intensity and vorticity for the non-scoured fixed bed base. Melville [13] and Melville and Raudkivi [3] studied the relationship between horseshoe vortex and scour hole. Qadar [14] and Sarker [15] studied the flow characteristics around cylindrical piers on a scoured bed. Ahmed and Rajaratnam [16] worked on smooth, rough and mobile beds to examine the velocity distribution around the circular pier. Istiarto [17], Dey and Raikar [18] and Das et al. [19] have experimentally determined the velocity, turbulence intensity, turbulent kinetic energy and bottom shear stress distribution around the circular bridge. Unger and Hager [6] used Particle Image Velocimetry (PIV) in their study. Barbhuiya and Dey [20] measured the turbulent flow field at a vertical semicircular cylinder with a flat plate attached to the sidewall of a rectangular channel and at a wing-wall abutment. Yulistiyanto [4] investigated the velocity field around a cylindrical bridge pier in various planes while there is no scour and Istiarto [17] made relevant measurements under equilibrium scour. Akib et al. [21] focused on the relationship between scour depth in complex pier groups and combined piles bridge and various parameters including the variation of inflow velocity, distance, and time.

In nature, unsteady flows are the most common type of open channel flow. The flow features like average velocity, and turbulence intensity. Reynolds stress [22-27], the suspended material [28] and the bed load [29-32] are the issues investigated in unsteady flow conditions [33-35].

Studies related to bridge piers under unsteady flow conditions are relatively scarce [36-38], particularly the investigations on the velocity and turbulence characteristics in the presence of a bridge pier [39]. To the authors knowledge, experimental studies dealing with the velocity variation with time–on the presence of the bridge piers for unsteady flow is scarce. Gargari et al. [40] investigated the flow passed a circular pile in gradually-varied unsteady flow. Erdog [41] and Erdog et al. [42] investigated the hysterical effects in flow structure behind a finite array of cylinders under gradually varying unsteady flow conditions. Therefore, it was decided to conduct an experimental study dealing with the velocity variation with time in front of the bridge piers for unsteady flow. In this study, the time variation of instantaneous velocity was investigated at clear-water and unsteady flow conditions in a water column in front of the

piers. Three cases were taken into consideration namely, without a pier, with a pier having a diameter of 6 cm, and a pier with a diameter of 9 cm. The variation of mean and fluctuating components of the velocity and the reduction in velocity due to the presence of the pier were calculated and interpreted.

2. Experimental Setup and Procedure

The experiments were conducted in a rectangular recirculating flume of 0.7 m wide (B) and 18 m long, having a slope of 0.004 (Fig. 1). The bed was composed of cohesionless sediment with a median diameter d_{50} = 0.43 mm. The total sediment depth was 22 cm and sediment transport was not observed during the experiments. Coarse sediments were placed at the bed surface of the first 1.7 m of the flume in order to develop a fully turbulent flow and to prevent the local scour at the entrance of the flume [43, 44].

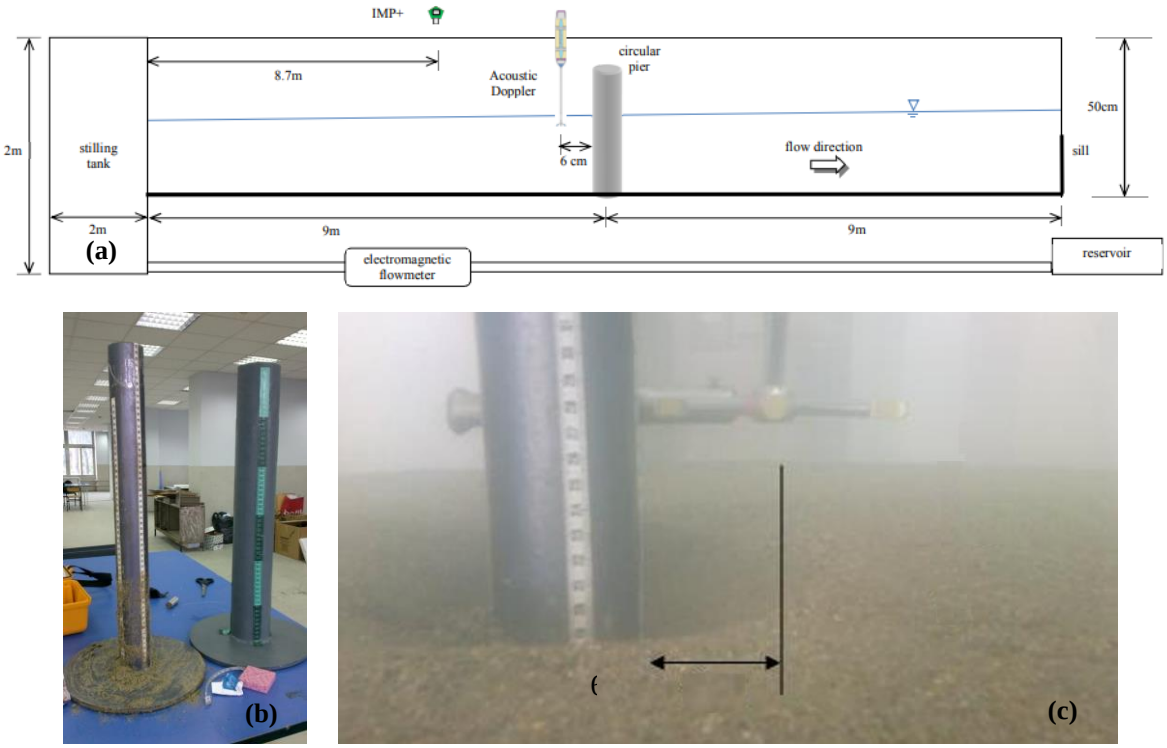

Figure 1.(a) Scheme of the experimental set-up, **(b)** piers, **(c)** location of the Flow Tracker

The flow rate in the flume was adjusted using a pump speed control unit (PSCU). The hydrographs were generated by increasing and/or decreasing the revolution rate of the pump as a percentage at desired time increments with this device. The advantage of the well-known fact was taken that the pump speed of a pump and the flow rate are directly and linearly proportional with each other.

Three triangular shaped asymmetrical hydrographs namely U1, U2 and U3 with rising durations of 1.5 min, 4.5 min and 9 min were generated. The falling duration of all experiments was the same and it was 1 minute.

The instantaneous point velocities were measured by a side looking ultrasonic instrument (Flow Tracker, Sontek) at x = 8.94 m where x is the distance from the flume entrance. To obtain the velocity time series at various locations within the flow depth, the instrument was first fixed at a specific location above the original sediment bed level and the hydrograph was generated and the velocity was measured throughout the duration of the hydrograph. Then the instrument was shifted to a neighboring vertical location, the same hydrograph was generated, and another velocity time series related to this neighboring point with a different height from the bottom sediment bed is obtained. The hydrograph generation at each vertical location is denoted as a run and resulting with a time series particularly for that elevation.

The velocity measurements were realized at the location of the bridge pier prior to its installation. Each experiment conducted in the absence of bridge piers was denoted by "a". This step is aimed at obtaining velocity data of the flow unperturbed by the cylinder. The data serve as a reference with which the measured data around the cylinder shall be compared. Two circular piers with diameters of b = 6 cm and b = 9 cm were used in the flume located at x = 9 m. The experiments with a pier diameter of 6 cm were denoted as "b" and with a pier diameter of 9 cm as "c". The velocity measurements were taken 6 cm upstream of the bridge pier. It was noted that the velocity measurements at points closer about 4.5 cm to the pier were not possible.

The variation of approach flow depth with time was measured at (B-b)/2 upstream part of the piers according to Oliveto and Hager [45], which was 8.7 m from the entrance by means of an ultrasonic level meter with a precision of 1 mm. The flow rate was measured by an electromagnetic flow meter mounted on the pipe for each run and averaged to determine the time variation of the flow rate for one experiment.

3. Methodology for Data Treatment

For the treatment of velocity time series in the stream-wise and vertical axis, the following procedure and equations were adopted.

The instantaneous point velocities $u(t)$ and $w(t)$ can be decomposed into their time-varying mean values $\bar{u}(t)$ and $\bar{w}(t)$, and their fluctuating components as $u'(t)$ and $w'(t)$ in longitudinal (x-axes) and vertical (z-axes) directions, respectively, as given in Eq. (1.a) and Eq. (1.b).

$$u(t) = \bar{u}(t) + u'(t) \tag{1.a}$$

$$w(t) = \bar{w}(t) + w'(t) \tag{1.b}$$

where (t) denotes the variable as a function of time as for the unsteady flows.

The obtained instantaneous point velocity time series $u(t)$ at each vertical location were smoothed by using the moving average algorithm to get the time varying mean $\bar{u}(t)$ and the fluctuating components $u'(t)$. The mean value at any instant was calculated by taking the average of the previous and proceeding 10 data as in Eq. (2). Same procedure was applied to calculate the $\bar{w}$(t) and $w'(t)$.

$$\bar{u}_n = \sqrt{\frac{1}{21}\sum_{i=n-10}^{n+10} u_i} \tag{2}$$

The turbulence intensity of the stream-wise and vertical velocities are determined by calculating the root-mean-square (rms) of the fluctuating component which also has a time varying character. The rms(u) and rms(w) for nth data were calculated by taking the mean average of the previous and proceeding 10 data as

$$\left[\, rms(u) \,\right]_n = \sqrt{\frac{1}{21}\sum_{i=n-10}^{n+10} \left(u_i - \bar{u}_i\right)^2} \tag{3}$$

Reynolds stress, τ can be calculated by the equation given below,

$$\boldsymbol{\tau = -\rho\overline{u'w'}} \tag{4}$$

where the u' and w' are the fluctuating components, ρ is the density of water.

4. Experimental Results

For all experiments, the base values of flow depth h_{base}, flow rate Q_{base} and mean velocity V_{base} were 12.2 cm, 2.1 L/s and 2.4 cm/s, respectively. The variation of the flow rate with time is depicted in Fig. 2. Table 1 gives details of the experiments in which Q_{peak} and h_{peak} are the peak values of flow rate and flow depth. Time to the peak value of the flow rate is denoted by $t_{r\,Q}$. Since the same hydrograph is measured for all cases a, b, and c, the peak values of flow rate are the same.

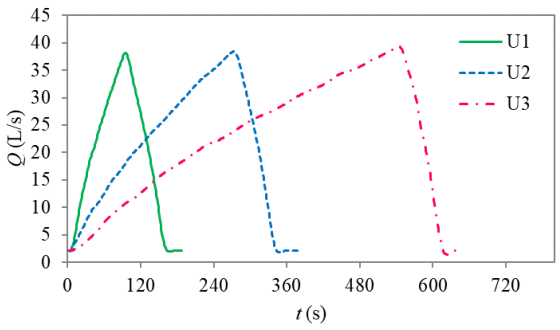

Figure 2. Variation of flow rate with time.

Table 1.The peak values of flow rate and flow depth, time to peak value of flow rate and the unsteadiness parameter.

Parameter	U1	U2	U3
Q_{peak} (L/s)	38.2	38.4	39.3
h_{peak} (cm)	19.5	20.6	20.8
$t_{r\,Q}$ (s)	96	273	544
α	0.0049	0.0021	0.0011

The unsteadiness of a hydrograph can be defined by the change of flow depth within a specified time interval [22]. The dimensionless unsteadiness parameter α, as given below, was proposed by Nezu and Nakagawa [46] and used by Nezu et al. [22], Onitsuka and Nezu [47] and Nezu and Sanjou [48].

$$\alpha = \frac{1}{U_c}\frac{\Delta h}{t_{r\,Q}} \tag{5}$$

where $\Delta h = h_{peak} - h_{base}$, $U_c = (V_{base} + V_{peak})/2$, V_{peak} is the peak mean velocities. Nezu and Sanjou [42] divided the open channel flows into two categories, as if $\alpha < 0.001$, then the flow is considered as low unsteady flow otherwise it has high unsteadiness characteristics [22].

The variation of instantaneous point velocities with time and time-varying means denoted as raw and smoothed data of experiments U2b measured at z/h_{base} = 0.45 are depicted in Fig. 3. The negative vertical velocity values indicate the down-flow towards the bed.

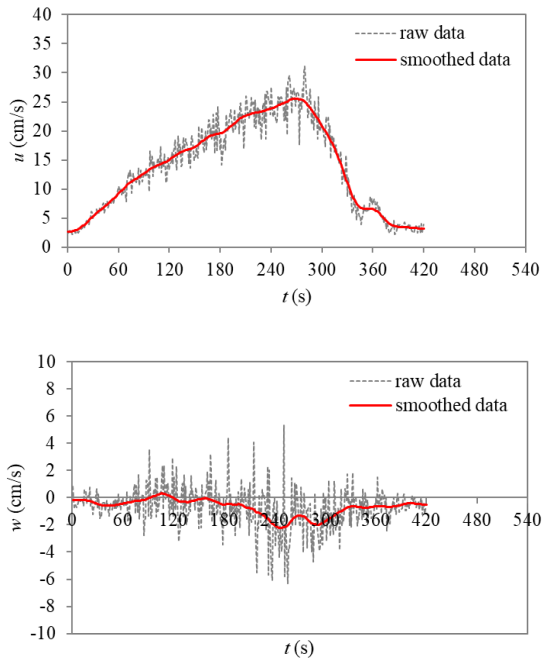

Figure 3. Variation of instantaneous point velocities and their time varying mean values.

The maximum velocity values of the smoothed data were obtained from each time series through the water column. The peak values of the time time-varying mean velocities for the cases without a pier, with small pier (b = 6 cm) and big pier (b = 9 cm) are calculated and given in Table 2, for z/h_{base} = 0.4 and z/h_{base} = 1.0.

Table 2. The peak values of the time-varying mean velocities for the cases without a pier and with the piers of diameter b = 6 cm and b = 9 cm (All velocity values are in cm/s).

peak value	z/h_{base}	U1a	U1b	U1c	U2a	U2b	U2c	U3a	U3b	U3c
$\overline{u}$	0.4	23.70	22.93	20.34	26.05	24.05	22.90	27.79	24.10	23.36
	1.0	28.84	23.62	22.73	30.10	26.05	25.31	30.58	26.09	23.80
$\overline{w}$	0.4	-0.91	-1.93	-2.62	-1.07	-1.77	-2.59	-1.36	-2.73	-3.11
	1.0	-1.23	-1.33	-2.53	-1.10	-1.74	-2.20	-1.07	-2.31	-2.35

It is revealed that the maximum value in the stream-wise direction decreases with the presence and even with the increase in pier diameter for stream-wise direction at all depths. The maximum value in the vertical direction on the other hand, increases its magnitude as a downflow. The stream-wise velocities are all greater near the surface than the ones near the bed. The maximum values of vertical velocity are the same at all depths for most of the experiments. A prominent effect of the unsteadiness on the maximum values was not noted.

The stream-wise velocity profiles are given in Fig. 4, at various dimensionless times as $t/t_{r\,Q}$ equal to 0.25, 0.50 and 1.0 as peak time. The flow depth for U3 experiments is the highest for the corresponding time of other U2 experiments and U1 experiments.

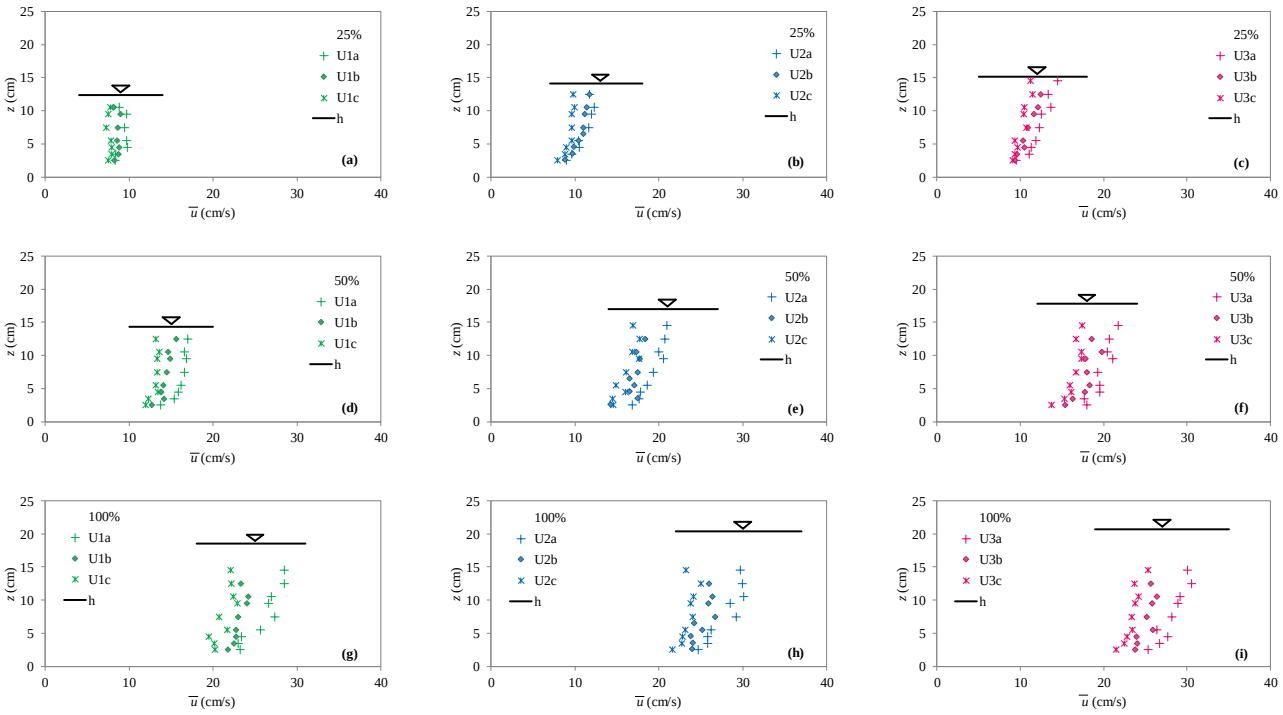

Figure 4. Velocity profiles in longitudinal direction t/t_{rQ} = 0.25 for (a) U1, (b) U2, (c) U3, 0.50 for (d) U1, (e) U2, (f) U3, 1.0 for (g) U1, (h) U2, (i) U3.

It is revealed that for all hydrographs, the presence of the bridge pier results in a retardation of the point velocities. For all dimensionless times, it is observed that the hydrograph U1 has the velocity profile having the lowest velocity values, whereas the profiles in U2 and U3 are greater. As seen from the graphs, the greater the diameter of the pier is, the steeper the velocity profile is. The maximum value of the point velocity occurred at a vertical elevation z equal to around 12.5 cm for most of the experiments. This is in accord with Song and Graf [49] who revealed that the maximum velocity occurs below the water surface.

Song and Graf [49] revealed that during the passage of the hydrograph, the velocities in the rising limb are greater than the ones in the falling limb for equal depths. The velocity profiles of the same flow depth regarding the rising and falling durations are depicted in Fig. 5. The flow depth of 16 cm was selected since it is the average base and peak flow depths and occurs at t = 62 s, 108 s, 170 s in the rising and t = 165 s, 348 s, 620 s in the falling limbs of the experiments U1, U2, and U3, respectively. It is observed that for the same depth, the profiles in the rising limb are always greater than the falling limb. This is more prominent for the ones with higher unsteadiness, particularly for U1. The effect of the presence of the bridge pier retards the flow resulting in more uniform, steeper, and small velocity profiles.

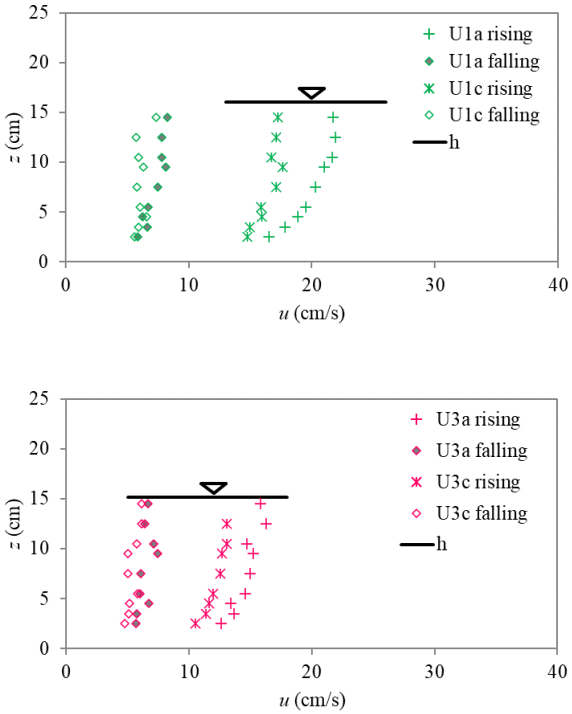

Figure 5. Velocity profiles in longitudinal direction of same flow depth (a) U1a & U1c and (b) U3a & U3c, without a pier and with 9 cm pier, respectively.

The velocity profiles of vertical component w at the dimensionless times 0.5 and 1.0 are depicted in Fig. 6 for U2 experiments. It is observed that in the absence of the bridge pier, the average vertical flow is nearly equal to zero in the water column. The presence of small pier increases the magnitude of the down flow prominently greater near the bed. These results are concluded for other experiments as well.

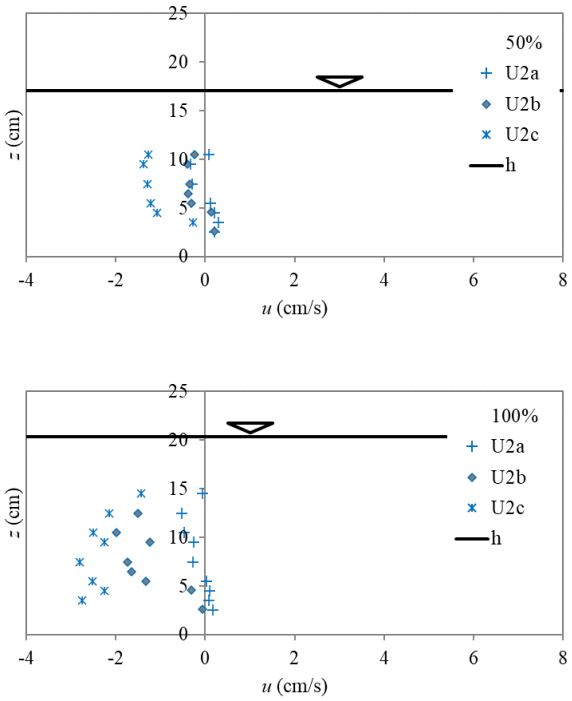

Figure 6. Velocity profiles in vertical direction at the dimensionless times (a) 0.5 and (b) 1.0.

The time variation of the fluctuating component of stream-wise and vertical velocities are calculated for U3a at z/h_{base} = 0.4 and z/h_{base} = 1.0 and for U3c at z/h_{base} = 0.4 as given in Fig. 7a, 7b and 7. c, respectively, as an example. The negative values are due to the decrease in instantaneous velocity with respect to mean velocity, whereas the positive values represent the increase. As depicted in Fig. 7.a and 7. c, both *u*' and *w*' have an increasing characteristic with time in the rising duration. In order to analyze this result, the rising duration was divided into three equal time intervals, namely the initial, middle, and peak phases. The band limits are depicted on the same figure as the extreme values i.e. minimum and maximum. The standard deviations were calculated within each time interval and summarized in Table 3 and Table 4 for z/h_{base} = 0.4 and z/h_{base} = 1.0, respectively, including the falling duration. The extreme bands become wider in time for z/h_{base} = 0.4 whereas this is not observed at locations near the water surface. The standard deviation for the fluctuating values of *u*' and *w*', are depicted in Fig 7. a and 7 .c, in blue and orange colors respectively for each phase. The standard deviation values did not differ for the initial, middle, and peak values for both stream-wise and vertical velocities near the surface. As illustrated in Fig 7 .b, the average standard deviation for three phases are 1.80 cm/s and 1.43 cm/s, for *u*' and *w*', respectively. For most of the experiments, the standard deviation is in general less than the one corresponding to peak time. The presence of the pier did not considerably change this behavior of the fluctuation components close to the water surface (Table 4) whereas the standard deviation of stream-wise component is suppressed for those close to bed (compare Fig 7.a and 7. c).

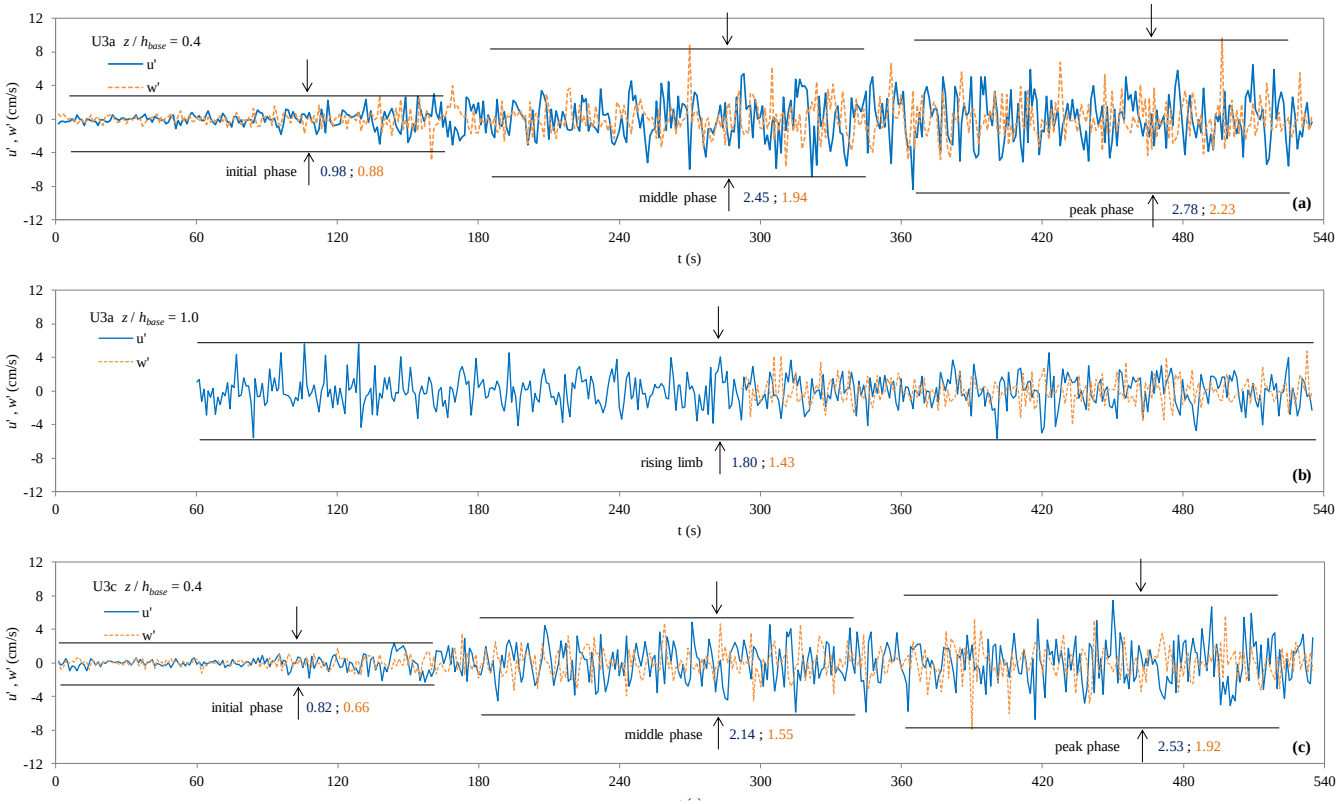

Figure 7. Variation of u ' and w ' with time (a) U3a at z/hbase = 0.4, (b) U3a at z/hbase = 1.0, and (c) U3c at z/hbase = 0.4

The standard deviation values calculated for the time intervals at z/h_{base} = 0.4.

	u'				*w'*			
	initial	middle	peak	falling	initial	middle	peak	falling
U3a	0.98	2.45	2.78	1.72	0.88	1.94	2.23	2.51
U3b	1.09	2.00	2.74	2.39	0.86	1.82	2.38	1.79
U3c	1.97	2.14	2.53	2.25	1.48	1.55	1.92	1.34
U2a	0.73	2.04	3.07	1.68	0.66	1.76	1.65	1.38
U2b	0.72	2.32	2.86	2.09	0.80	1.87	2.47	1.85
U2c	0.64	1.96	2.79	2.76	0.46	1.61	1.95	1.83
U1a	1.50	1.24	2.47	2.19	0.39	1.47	2.20	1.76
U1b	1.17	1.16	2.74	2.04	0.25	1.12	1.90	1.48
U1c	1.17	0.84	2.87	2.52	0.39	1.47	2.20	1.80

The standard deviation values calculated for the time intervals at z/h_{base} = 1.0.

	u'				w'			
	initial	middle	peak	falling	initial	middle	peak	falling
U3a	1.84	1.72	1.82	1.49	-	1.48	1.39	1.30
U3b	1.60	1.67	1.81	1.56	-	1.35	1.40	1.17
U3c	1.67	1.56	1.94	1.54	-	1.09	1.57	1.31
U2a	1.89	1.77	1.62	1.47	-	1.35	1.34	1.13
U2b	1.90	1.86	1.58	1.65	-	-	1.40	1.57
U2c	1.52	1.67	1.81	1.14	-	1.52	1.45	1.28
U1a	-	-	1.81	1.45	-	-	1.23	1.56
U1b	-	-	1.94	1.70	-	-	1.14	1.94
U1c	-	-	1.63	1.76	-	-	1.23	1.22

The obtained time variation of stream-wise rms(u) and vertical rms(w) point velocities for all experiments corresponding to the elevation z/h_{base} = 0.4 are shown in Figs. 8.a,b,c and Figs. 8.d,e,f, respectively. It is observed that the presence of the piers did not have an influence on rms(u) or rms(w). The rms(u) values increase the rising limb and decrease in the falling limb. The turbulence intensity in the stream-wise direction attenuates when approaching the bed surface. Neither the presence of the pier nor the unsteadiness affected the intensity near the surface and near the bed. For the vertical velocity case, the rms(w) had a constant value throughout the hydrograph duration. In this direction, the intensity attenuates when approaching the bottom while remaining the same near the surface with the increase in pier diameter.

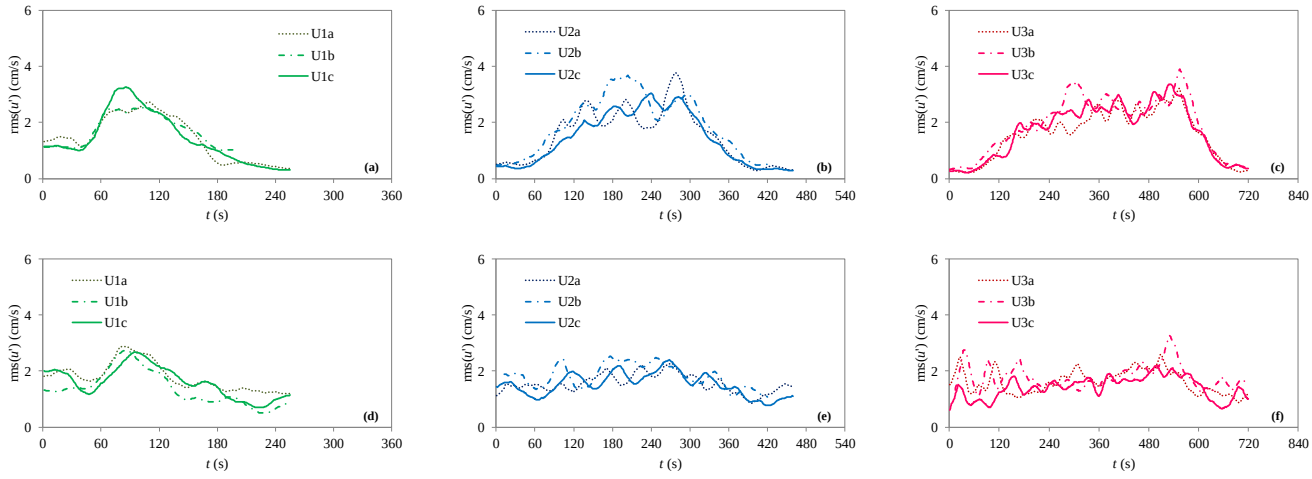

Figure 8. Variation of (a), (b) and (c) rms(u) with time for U1, U2 and U3, respectively and (d), (e) and (f) rms(w) with time for U1, U2 and U3, respectively.

The variation of u' with w' is plotted for U2 and U1 in Fig. 9, considering the initial, middle and peak phases additionally the falling phase. For all cases, the sweep and ejection events dominate throughout the hydrograph. In all graphs, it is also observed that the fluctuation values in the stream-wise direction are all greater than the ones in the vertical direction.

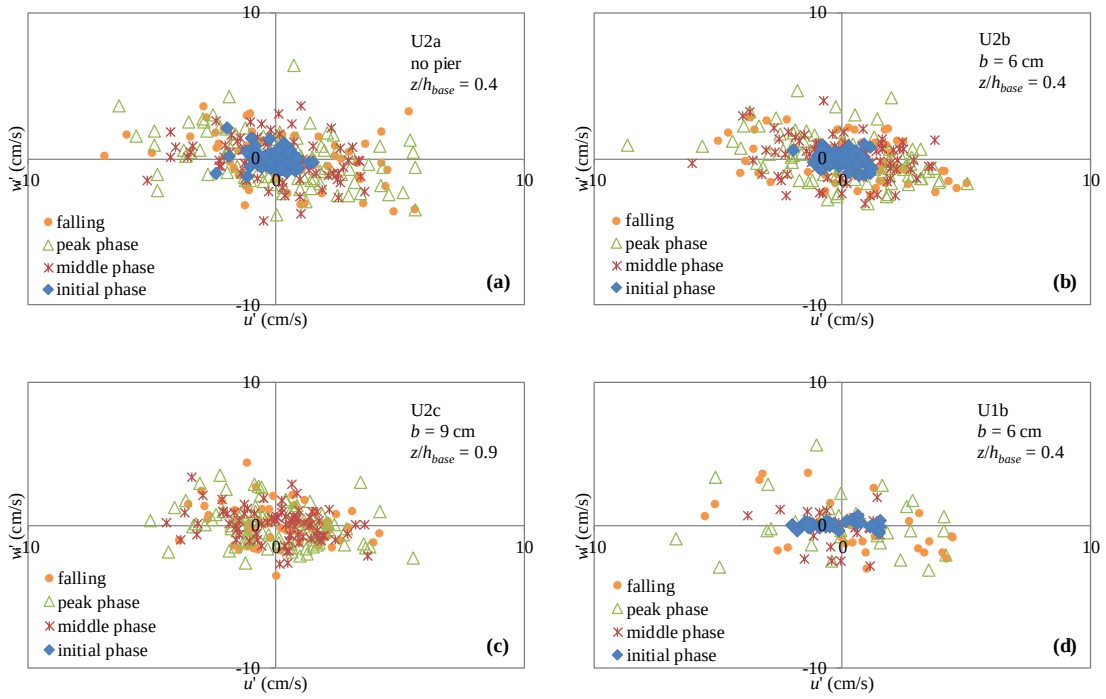

Figure 9. The variation of *u* ' with *w* 'for (a) U2a, (b) U2b, (c) U2c, (d) U1b.

By using the fluctuating components, the time variation of *u*'*w*' is calculated and given in Fig 10. Whether there is a pier or not the *u*'*w*' has its maximum value near the bottom and decreases towards the water surface. For all the experiments, the *u*'*w*' increases in the rising limb and decreases in the falling limb. The unsteadiness of the hydrograph did not affect considerably but the presence of the pier decreased the maximum values of the *u*'*w*'.

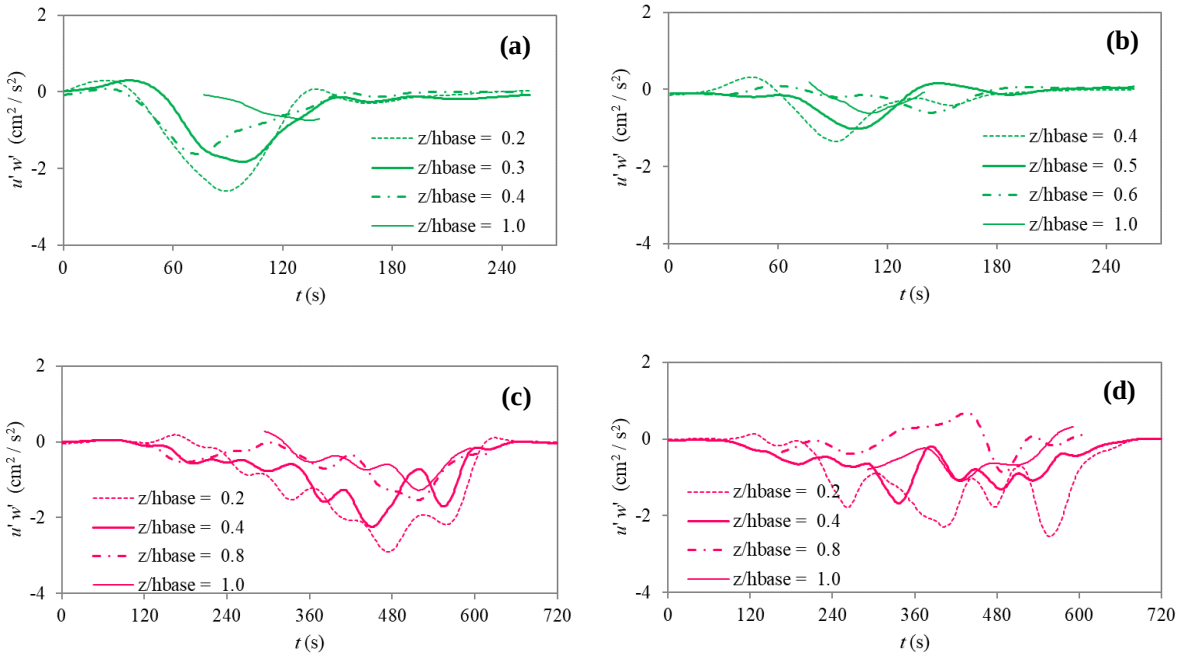

Figure 10. The time variation of *u* ' *w* ' for (a) U1a, (b) U1c, (c) U3a, (d) U3c.

The presence of the pier decreased the velocity in stream-wise and increased the down flow velocity in the vertical direction as depicted in Fig. 11.a and 11.b, respectively. The average differences for cases b and c were calculated as subtracting the time average velocity value at a specific time from that of corresponding to the case a. Therefore, the curves are given only for experiments b and c as time variation of avg($\overline{\Delta u}$) and avg($\overline{\Delta w}$). It is observed that the unsteadiness of the hydrograph did not influence the average change in the stream-wise. The maximum average reduction for pier width of 6 cm is 3.1 cm/s (average of 3.1 cm/s, 3.3 cm/s and 3.0 cm/s for U1b, U2b and U3b, respectively) and 4.3 cm/s (average of 4.4 cm/s, 4.3 cm/s and 4.2 cm/s for U1c, U2c and U3c, respectively) for the pier width 9 cm in stream-wise direction. The corresponding maximum percent changes at peak were calculated as 6% and 11%. In vertical direction, the maximum average increase in down-flow was calculated as 0.5 m/s and 1.5 cm/s for the small and big piers.

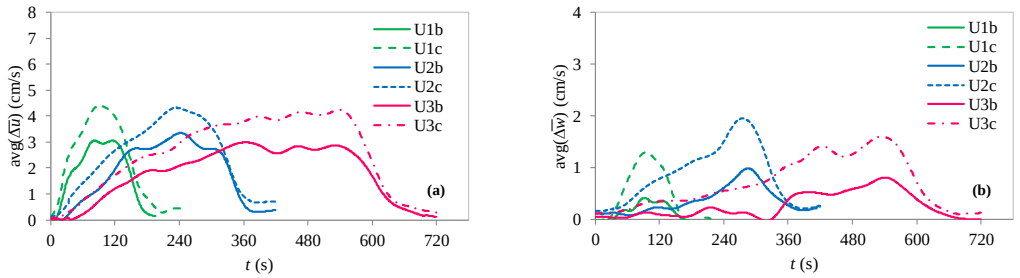

Figure 11. Average reduction in maximum velocity due to the presence of pier (a) in stream-wise and (b) vertical directions.

The reductions in point velocities at peak are calculated and given in Fig. 12. It is revealed that the reduction increases with *z* due to both piers but prominently for the pier with *b* = 9 cm for the velocity in stream-wise direction. The increase in down-flow does not change with depth but is greater for the pier with a greater diameter.

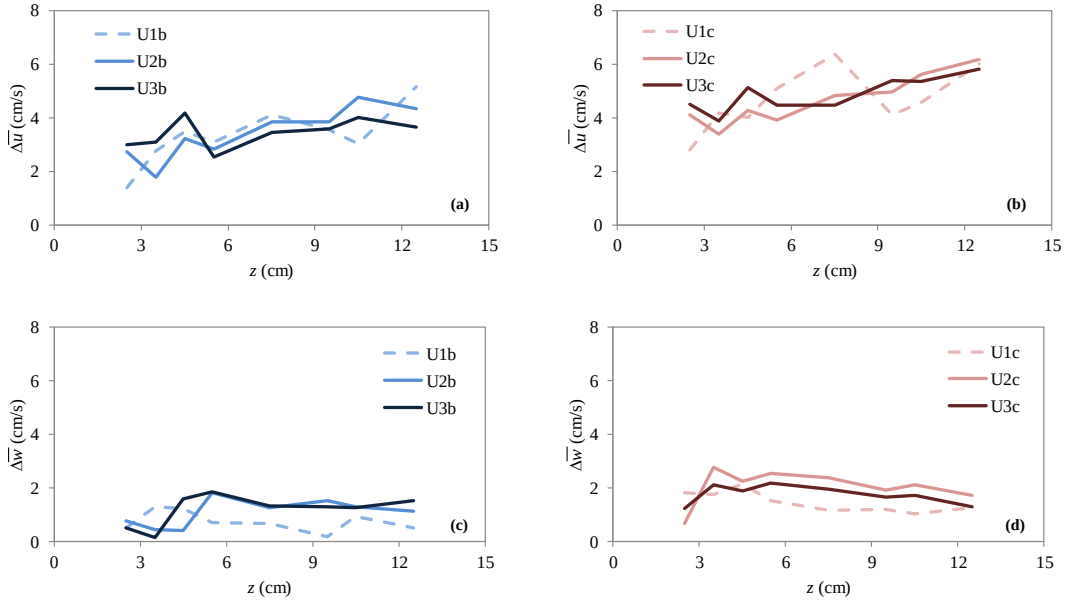

Figure 12. Variation of change in maximum velocity due to presence of pier with depth, (a) 6 cm pier diameter and (b) 9 cm pier diameter in stream-wise direction and (c) 6 cm pier diameter and (d) 9 cm pier diameter in vertical direction.

5. Conclusion

The time variation of point velocities in a stream-wise and vertical direction at a point upstream of a bridge pier were investigated at clear-water conditions under unsteady flow conditions. Three triangular-shaped hydrographs with approximately the same peak discharges but with different rising durations were generated. The effect of two circular bridge piers which are 6 cm and 9 cm in diameter on the flow properties was discussed in which the measurements were also conducted in the absence of any pier. The main findings can be summarized as follows;

- The presence of the pier decreased the stream-wise velocity while increasing the magnitude of vertical velocity towards the bed, prominently greater near the bed.
- The greater the diameter of the pier is, the steeper the stream-wise velocity profiles are.
- It was observed that for the same depth, the profiles in the rising limb are always greater than the falling limb. This is more prominent for the ones with higher unsteadiness.
- The standard deviation of the stream-wise fluctuating components near the bed increases in the rising limb with time, while it remains constant near the surface.
- The standard deviation of the vertical velocity fluctuating components did not differ throughout the hydrograph duration. The presence of the pier did not considerably change this behavior.
- The sweep and ejection events dominate throughout the duration of all hydrographs.
- For all the experiments, the $u'w'$ increase in the rising limb and decrease in the falling limb. Whether there is a pier or not the $u'w'$ has its maximum value near the bottom and decreases towards the water surface. The presence of the pier certainly decreased the maximum values of the $u'w'$.
- The maximum percent reduction at peak flow was calculated as 6% and 11%, for the piers with a width of 6 cm and 9 cm, respectively.
- The reduction in stream-wise point velocities at peak flow increases with depth. The greater the pier diameter is, the more the reduction is.
- The change in a vertical direction at peak flow due to the pier is constant throughout the depth.
- The results of this study could be used to verify the numerical studies for unsteady flows with bridge piers.

In future studies, the flow conditions and turbulence structures around the bridge piers can be determined by using symmetrical and asymmetrical hydrographs with different unsteadiness and by using different bridge pier diameters with different shapes and different types of sediments. The evolution of coherent structures under unsteady flow conditions would be a novel topic in this field.

Acknowledges

The author would like to express her gratitude to Prof. Dr. Şebnem ELÇİ for supplying the ultrasonic velocity meter used during the execution of the experiments.

List Of Notations

avg($\Delta \bar{u}$) average value of the change in stream-wise velocity due to bridge pier [LT^{-1}];

avg($\Delta \overline{w}$) average value of the change in vertical velocity due to bridge pier [LT^{-1}];

b bridge pier diameter [L];

B flume width [L];

d_{50} median size of sediment [L];

h_{base} flow depth at base flow [L];

h_{peak} flow depth at peak flow [L];

rms(u) root-mean-square of the velocity in stream-wise direction [LT^{-1}];

rms(w) root-mean-square of the velocity in vertical direction [LT^{-1}];

t time [T];

$t_{r\,Q}$ time to peak value of the flow rate [T];

u instantaneous point velocity in stream-wise direction [LT^{-1}];

u' fluctuating components of point velocity in stream-wise direction [LT^{-1}];

$\bar{u}$ time varying mean of point velocity in vertical direction [LT^{-1}];

w instantaneous point velocity in vertical direction [LT^{-1}];

w' fluctuating components of point velocity in vertical direction [LT^{-1}];

$\overline{w}$ time varying mean of point velocity in stream-wise direction [LT^{-1}];

x distance from the flume entrance [L];

z elevation from the bed surface [L];

U_c average of V_{base} and V_{peak} $U_c = (V_{base} + V_{peak})/2$ [LT^{-1}];

V_{base} approach velocity at base flow [LT^{-1}];

V_{peak} approach velocity at peak flow [LT^{-1}];

Q_{base} flow rate at base flow [L^3T^{-1}];

Q_{peak} flow rate at peak flow [L^3T^{-1}];

Δh difference between the base and peak flow depths [L];

$\Delta \bar{u}$ change in stream-wise velocity due to bridge pier [LT^{-1}];

$\Delta \overline{w}$ change in vertical velocity due to bridge pier [$L\,T^{-1}$];

α dimensionless unsteadiness parameter [-];

References

[1] Landers, M. N., (1992). Bridge Scour Sata Management. Published in Hydraulic Engineering: Saving a Threatened Resource—In Search of Solutions: *Proceedings of the Hydraulic Engineering sessions at Water Forum'92. Baltimore, Maryland*, August 2–6.

[2] Franzini, J. B. and Finnemore, E. J.(1997). *Fluid Mechanics with Engineering Applications*, (McGraw-Hill), ISBN 0-07-021914 1.

[3] Melville, B. W. and Raudkivi, A. J. (1977). Flow characteristics in local scour at bridge piers. *J. Hydraul. Res.*, 15 373–380.

[4] Yulistiyanto, B. (1997), Flow around a cylinder installed in a fixed-bed open channel, PhD thesis no 1631, École Polytechnique Fédérale de Lausanne, Switzerland.

[5] Breusers, H. N. C., Nicollet, G. and Shen, H. W. (1977). Local scour around cylindrical piers. *J. Hydraul. Res.*, 15: 211–252.

[6] Unger, J. and Hager, W. E. (2007). Down-flow and horseshoe vortex characteristics of sediment embedded bridge piers, *Experiments in Fluids*, 42: 1–19.

[7] Ettema, R., Kirkil, G. and Muste, M., (2006). Similitude of large scale turbulence in experiments on local scour at cylinders. *J. Hydraul. Eng*., 132: 33–40.

[8] Kirkil, G., Constantinescu, S. G. and Ettema, R. (2008). Coherent structures in the flow field around a circular cylinder with scour hole. *J. Hydraul. Eng*., 134: 572–587.

[9] Baker, C. J. (1979). Laminar horseshoe vortex. *J. Fluid Mech*. 95: 347–367.

[10] Baker, C. J. (1980). The turbulent horseshoe vortex. *Journal of Wind Engineering Industrial Aerodynamics*, 6 9–23.

[11] Baker, C. J. (1985). The position of points of maximum and minimum shear-stress upstream of cylinders mounted normal to flat plates. *Journal of Wind Engineering Industrial Aerodynamics*, 18: 263–274.

[12] Yulistiyanto, B. (2009). Velocity measurements on flow around a cylinder, *Dinamika Teknik Sipil*, 9: 111–118.

[13] Melville, B. W. (1975). Scour at bridge sites. Report No 117, School of Engineering, University of Auckland, Auckland, New Zealand.

[14] Qadar, A. (1981). The vortex scour mechanism at bridge piers. *J. Proc. of Inst. Civ. Engrs*, 71: 739–757.

[15] Sarker, M. A. (1998). Flow measurement around scoured bridge piers using Acourstic Doppler Velocimeter (ADV). *Flow Measurement and Instrumentation*, 9: 217–227.

[16] Ahmed, F. and Rajaratnam, N. (1998). Flow around bridge piers. *J. Hydraul. Eng.*, 124: 288–300.

[17] Istiarto, I. (2001). Flow around a cylinder on a mobile channel bed. Ph.D. Thesis, no. 2368, EPFL, Lausanne, Switzerland.

[18] Dey, S. and Raikar, V. R., (2007). Characteristics of horseshoe vortex in developing scour holes at piers. *J. Hydraul. Eng.*, 133: 399–413.

[19] Das, S., Das, R. and Mazumdar, A. (2013). Comparison of characteristics of horseshoe vortex at circular and square piers. *Research Journal of Applied Sciences, Engineering and Technology*, 5: 4373–4387.

[20] Barbhuiya, A. K. and Dey, S. (2003). Velocity and turbulence at a wing-wall abutment. *Sadhana*, 28: 35–56.

[21] Akib, S., Jahangirzadeh, A., and Basser, H. (2014). Local scour around complex pier groups and combined piles at semi-integral bridge. *J. Hydrol. Hydromech*., 62: 108–116.

[22] Nezu, I., Kadota, A. and Nakagawa, H. (1997). Turbulent structure in unsteady depth varying open-channel flows, *J. Hydraul. Eng*., 123 752–763.

[23] Song, T. (1994). Velocity and turbulence distribution in non-uniform and unsteady openchannel flow. PhD thesis no 1324, Ecole Polytechnique Fédérale de Lausanne, Switzerland.

[24] Tu, H. (1991). Velocity distribution in unsteady flow over gravel beds, PhD thesis no 911, École Polytechnique Fédérale de Lausanne, Switzerland.

[25] Bares, V., Jirak, J. and Pollert, J. (2008). Spatial and temporal variation of turbulence characterisitcs in combined sewer flow. *Flow Measurement and Instrumentation*, 19: 145–154.

[26] Bombar, G. (2016). The hysteresis and shear velocity in unsteady flows. *Journal of Applied Fluid Mechanics*, 9(2): 839–853.

[27] Khuntia, J. R., Devi, K., Khatua, K. K. (2021). Turbulence characteristics in a rough open channel under unsteady flow conditions, ISH Journal of Hydraulic Engineering, 27:sup1, 354-365, https://doi.org/10.1080/09715010.2019.1658549.

[28] de Sutter, R., Verhoeven, R. and Krein, A., (2001). Simulation of sediment transport during flood events: Laboratory work and field experiments. *Hydrological Sciences Journal*, 46: 599–610.

[29] Suzka, L. (1987). Sediment transport at steady and unsteady flow: a laboratory study, PhD thesis no 704, École Polytechnique Fédérale de Lausanne, Switzerland.

[30] Qu, Z. (2002). Unsteady open-channel flow over a mobile bed. PhD thesis no 2688, École Polytechnique Fédérale de Lausanne, Switzerland.

[31] Güney, M. Ş., Bombar, G. and Aksoy, A. Ö., (2013). Experimental study of the coarse surface development effect on the bimodal bed-load transport under unsteady flow conditions. *J. Hydraul. Eng*., 139: 12–21.

[32] Francalanci, S., Paris, E. and Solari, L., (2013). A combined field sampling-modeling approach for computing sediment transport during flash floods in a gravel-bed stream. *Water Resour. Res*., 49: 6642–6655.

[33] Nanson, G. C. (1974). Bed load and suspended load transport in a small, steep, mountain stream, *Am. J. Sci.*, 274 471–4

[34] Kuhnle, R. A. (1992). Bedload transport during rising and falling stages on two small streams, *Earth Surf. Proc. Land*., 17: 191–197.

[35] Çokgör, S. and Diplas, P. (2001).Bed load transport in gravel streams during floods. *Proceedings of World Water and Environmental Resources Congress, ASCE*, 1, 47.

[36] Lopez, G., Teixeira, L., Ortega-Sanchez, M. and Simarro, G. (2006). Discussion of 'Further results to time-dependent local scour at bridge elements'. *J. Hydraul. Eng.*, 132: 995–996.

[37] Lai, J. S., Chang, W. Y. and Yen, Y. L. (2009). Maximum local scour depth at bridge piers under unsteady flow. *J. Hydraul. Eng.*, 135: 609–614.

[38] Hager, W. H. and Unger, J. (2010). Bridge pier scour under flood waves. *J. Hydraul. Eng*., 136: 842–847.

[39] Bombar, G. (2014). Clear-water bridge scour under triangular-shaped hydrographs with different peak discharges, *Proceedings of River Flow 2014 Conferece, Laussanne, Switzerland*

[40] Erdog, E. (2014). The influence of unsteadiness degree on hydraulic characteristics in open channel flow. Istanbul Technical University Graduate School of Science Engineering and Technology, M.Sc. Thesis, May 2014, 356137.

[41] Gargari, M. K., Kırca V. S. Ö., Yagcı, O., (2022). Experimental investigation of gradually-varied unsteady flow passed a circular pile. Coastal Engineering, 168 (2021) 103926, https://doi.org/10.1016/j.coastaleng.2021.103926.

[42] Erdog, E., Yagcı, O., Kırca, V. S. Ö. (2022). Hysterical effects in flow structure behind a finite array of cylinders under gradually varying unsteady flow conditions. Journal of Ocean Engineering and Marine Energy, https://doi.org/10.1007/s40722-022-00229-y.

[43] Saçan, C., Çetin, O.K., Bombar, G., (2013). Investigation of the scour inception around a circular bridge pier. Proceedings of the Second International Conference on Water, Energy, and the Environment, ICWEE,Kusadası, Turkey September 21-24, 2013.

[44] Çetin, O. K., Saçan, C., Bombar, G., (2016). Investigation of the relation between bridge pier scour depth and vertical velocity component, Pamukkale Universitesi Muhendislik Bilimleri Dergisi, 22(6):427-432, https://doi.org/10.5505/pajes.2015.76768.

[45] Oliveto, G. and Hager, W. H. (2002). Temporal evolution of clear-water pier and abutment scour, J. Hydraul. Eng., 128: 811–820.

[46] Nezu, I. and Nakagawa, H. (1993). *Turbulence in open-channel flows*, IAHR Monograph Series, (A.A. 619 Balkema Publishers), Rotterdam, The Netherlands.

[47] Onitsuka, K. and Nezu, I. (1999). Effect of unsteadiness on von Karman constant in unsteady open channel flows. *D1-Turbulent Channel Flows with Macro Roughness Vegetation, 28 th Congress of IAHR, Graz, Austria, Conf. Proceedings*.

[48] Nezu, I. and Sanjou, M. (2006). Numerical calculation of turbulence structure in depth varying unsteady open-channel flows. *J. Hydraul. Eng.*, 132: 681–695.

[49] Song, T. and Graf, W. H. (1996). Velocity and turbulence distribution in unsteady open-channel flows. J. Hydraul. Eng., 122: 141–154.